# Glassy electrons at the first-order Mott metal-insulator transition

Shreya Kumbhakar, Saurav Islam, Zhiqiang Mao, Yu Wang, and Arindam Ghosh

Phys. Rev. B **106**, L201112 — Published 23 November 2022

DOI: 10.1103/PhysRevB.106.L201112

# Glassy electrons at the first order Mott metal-insulator transition

Shreya Kumbhakar[1,⋆], Saurav Islam[1,⋆,†], Zhiqiang Mao[2], Yu Wang[2], and Arindam Ghosh[1,3]
[1] *Department of Physics, Indian Institute of Science, Bangalore 560012, India*
[2] *Department of Physics, Pennsylvania State University,*
*University Park, Pennsylvania 16802, USA* and
[3] *Centre for Nano Science and Engineering, Indian Institute of Science, Bangalore 560012, India*

The Mott metal-insulator transition remains one of the most scrutinized concepts in condensed matter physics. However, the kinetics of the charge carriers at the transition, involving both orbital and spin degrees of freedom, still remains poorly understood. A perfect platform to distinguish between the role of such competing interactions is strongly correlated oxides offering rich phase diagrams, which we use here to address the electron kinetics at the transition. We show a critical slowing down of electron kinetics at the the first order metal to Mott insulator transition in the Ruddlesden Popper oxide $Ca_3(Ru_{0.9}Ti_{0.1})_2O_7$ using low-frequency noise in resistance fluctuations. Critical slowing down of the electron kinetics is manifested as an enhancement of noise by an order of magnitude at the transition with a large shift of the spectral weight to lower frequencies. The second spectrum of noise is frequency dependent, indicating the presence of correlated fluctuations which gets suppressed under the application of a magnetic field. Our experiments provide compelling evidence of the formation of a spin-glass phase at the transition in these systems.

Despite immense theoretical and experimental progress, metal-insulator transition (MIT) [1–3] still remains an active area of research [4–13]. These transitions can be driven by disorder, leading to Anderson insulators [14] or strong correlation leading to Mott insulators [1, 2, 15]. Mott insulators are particularly important because of potential application in diverse fields due to tunability of the phase transition with external parameters [10–12]. In real materials, however complex interplay of lattice, spin and orbital degrees of freedom makes the critical phenomena at Mott transition a matter of active discourse [16–19].An issue of fundamental interest is the electronic kinetics and the presence of glassy behaviour at the transition [20]. Although the slowing down of electron kinetics is generally predicted for second-order phase transitions, a general consensus regarding the nature of critical fluctuations near the first order Mott transition is lacking. Here we address these questions with a very careful set of measurements, in a carefully chosen material with a high transition temperature, where quantum interference/localisation effects do not not dominate. Critical slowing down of electrons has been observed in organic salts [21] at temperature ($T$)≈ 34 K, but its nature in a crystalline solid where both orbital and spin degrees of freedom have competing strengths is not known. Experiments involving 3D doped semiconductors [22], disordered oxide films, 2D electron gases in MOSFETs [23], etc. have also claimed glassy electron kinetics at the transition, but most of them were carried out at low temperature where localization effects due to quantum interference were also rather strong. Additionally, electron kinetics at Mott transitions at high temperatures, for example in perovskite class of oxide films or rare-earth nickelates [24–26] become difficult to explore due to emergent spatial inhomogeneity at the transition.

The Ruddlesden-Popper (RP) ruthenate $Ca_3(Ru_{0.9}Ti_{0.1})_2O_7$ [27] is an excellent platform to understand the generality of electron kinetics at the Mott transition, where one can attempt to distinguish between the roles of orbital and spin degrees of freedom close to the critical temperature, which can be as high as ≈ 110 K. RP-type ruthenates [28] are a natural playground to observe rich correlated behavior, where physical parameters like doping, temperature, pressure and electric-field affect the distortion of $RuO_6$ octahedra, leading to drastic changes in magnetic and electrical properties of the system. Recent work in such compounds have reported spin-triplet superconductivity in $Sr_2RuO_4$ [29, 30], field-tuned nematic electronic phase [31], itinerant ferromagnetism [32, 33], antiferromagnetic (AFM) Mott insulating state [34], and paramagnetic "bad" metallicity [35]. $Ca_3Ru_2O_7$ is a RP-type compound, which undergoes two phase transitions [36, 37], a Neel transition from metallic paramagnetic (PM) phase at high temperature ($T$) to metallic a-AFM phase below $T = 56$ K and a structural phase transition to b-AFM phase below $T = 48$ K, where the in-plane resistivity increases and the spin orientation switches from the a-axis to the b-axis. Isovalent Ti doping into the Ru sites disrupts hopping of carriers in $Ca_3(Ru_{1-x}Ti_x)_2O_7$ and results in a bandwidth-controlled Mott transition from metallic PM phase to insulating G-AFM phase for $x > 0.05$ [27, 38]. However within a narrow range of magnetic field ($B$) and $T$, stripe like metallic domains has been observed in $Ca_3(Ru_{0.9}Ti_{0.1})_2O_7$ [39], which is believed to be $a/b$ - AFM phase, although its nature and role in the transition is yet to be investigated. Presence of competing interactions in $Ca_3(Ru_{0.9}Ti_{0.1})_2O_7$ [27] like intrabilayer ferromagnetic ordering due to itinerant charge carriers and superexchange AFM interations leads to a novel critical phenomena associated with the transition and the possibility of co-existence of multiple phases known as phase separation [40].

In this manuscript, we probe the collective behavior at the phase transition in $Ca_3(Ru_{0.9}Ti_{0.1})_2O_7$ with low

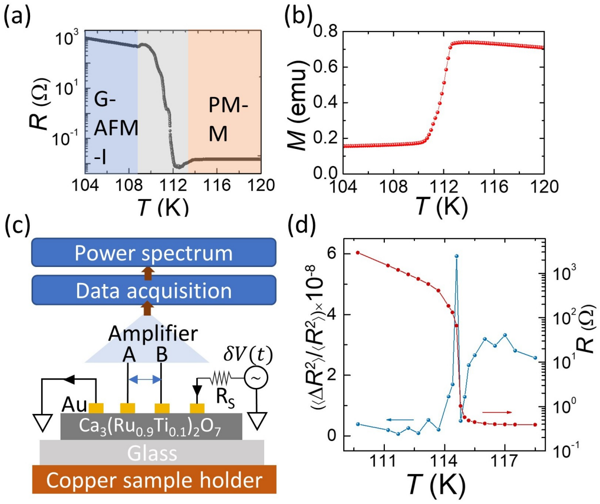

FIG. 1. Characterization of $Ca_3(Ru_{0.9}Ti_{0.1})_2O_7$ (a) Resistance ($R$) versus temperature ($T$) showing metal (M) to insulator (I) transition at $T \approx 112$ K. Blue and red regions indicate insulating G-antiferromagnetic (G-AFM-I) and metallic paramagnetic phases (PM-M) respectively. (b) Magnetization ($M$) versus $T$ data showing decrease in $M$ at $T \approx 113$ K from PM state to G-AFM state. (c) Schematic of the measurement circuit. (d) $T$-dependence of the normalized variance of resistance fluctuations ($\langle\Delta R^2\rangle/\langle R^2\rangle$) and $R$.

frequency resistance fluctuations [21, 22, 26, 41–45]. We observe an enhanced noise level across the transition, with a Lorentzian component superimposed on the $1/f^\alpha$ background. Our investigation reveals slowing down of the electron kinetics at the transition, causing significant rearrangement in the spectral weight distribution of noise. Strong non-Gaussianity observed in the second spectrum of noise suggests glassy kinetics at the transition. Application of $B$ suppresses this non-Gaussianity, indicating the formation of an intermediate spin-glass phase. Our experiment provides unambiguous signatures of emergent glassy kinetics of electrons across the Mott MIT in $Ca_3(Ru_{0.9}Ti_{0.1})_2O_7$ at finite $T$.

The $T$-dependence of the resistance ($R$) while slowly heating the single crystal (sample S1) of $Ca_3(Ru_{0.9}Ti_{0.1})_2O_7$ at 0.5 K/min (Fig. 1(a)) clearly exhibits metal to insulator transition at $T \approx 112$ K, with $R$ increasing by almost five orders of magnitude [See Supplementary information (SI) Sec. I for device details]. We have indicated three different regions according to the kinks observed in $R - T$ [39]. The crystal has a PM state above 113.5 K (red region, Fig. 1(a)) and G-type AFM state below 109 K (blue region, Fig. 1(a)). However very close to the transition between 109 K to 113.5 K (grey region, Fig. 1(a)) the system could be in a mixed phase (Fig. 1(a)). Fig. 1(b) shows sharp reduction in magnetization ($M$) when the crystal undergoes a transition from PM metallic phase to G-AFM insulating phase [39].

Low frequency $1/f$ noise measurements were performed by capturing four-probe ac voltage fluctuations with a lockin amplifier, with each block of data being recorded for 40 minutes with 1000 data points/sec, followed by digital signal processing to obtain the power spectral density (PSD, $S_V(f)$, $f$ is the spectral frequency) (Fig. 1(c)) [26, 46, 47]. The quadratic dependence of $S_V(f)$ with bias across the sample ($V$) was checked in both metallic and insulating regimes, ensuring that the measurements were performed in the linear Ohmic regime [See SI Sec. II] [48]. The stability of $T$ was maintained within 1 mK, eliminating fluctuation of $T$ as a possible origin of the excess noise [See SI Sec. III].

The $T$-dependence of normalized variance of resistance fluctuations, obtained by integrating the PSD over the experimental bandwidth ($f_{max}$ and $f_{min}$ are maximum and minimum frequencies respectively)

$$\frac{\langle\Delta R^2\rangle}{\langle R^2\rangle} = \int_{f_{\min}}^{f_{\max}} \frac{S_V(f)}{V^2} df \tag{1}$$

is shown in Fig. 1(d). We observe a sharp peak in $\langle\Delta R^2\rangle/\langle R^2\rangle$ across the transition, where it increases by an order of magnitude. We estimate the phenomenological Hooge parameter, $\gamma_H \approx 10^9$ [49] [See SI Sec. IV]. Although in conventional bulk and low dimensional systems, $\gamma_H \approx 10^{-5} - 1$ [41, 45, 47, 48, 50–60], such high values have been observed in MIT and attributed to percolation or glassy kinetics ( [22, 24–26, 61, 62].

To gain a better understanding of the origin of the peak in noise and large $\gamma_H$, we performed noise measurements at more closely spaced $T$ interval of 50 mK, near the transition ($T_c = 111.75$ K). Since the $R - T$ data showed hysteresis with $\Delta T_c \sim 1 - 2$ K between forward and reverse thermal cycles, we have plotted the data with respect to the shifted temperature $T - T_c$, where $T_c$ is the transition temperature of the corresponding thermal sweep. Representative time ($t$) dependence of $R$, close to the transition, is shown in Fig. 2(a) from $T = 111.75$ K ($T_c$) to $T = 111.45$ K ($T_c - 0.35$ K). It is evident that $R$ fluctuates between "high" and "low" states at specific $T$s. Such two level fluctuations (TLF) or random telegraphic noise (RTN) have been observed before in different physical systems such as MOSFETs and perovskite manganites, attributed to trapping-detrapping of carriers between defect levels and thermally activated switching between coexisting phases [63–66].

Expectedly, at $T$ where TLF are predominant, we find the noise magnitude to be high and the spectrum deviates strongly from $1/f^\alpha$ nature. Noise measurements in sample S2, taken at a resolution of 20 mK, also shows TLF and similar qualitative data [See SI Sec. V and VI]. PSD due to a dynamical process like activated fluctuation between two states with a single relaxation time $\tau_0$ and relaxation function $\propto \exp(-t/\tau_0)$, simplifies to a Lorentzian distribution [67]. Hence, we fit the normalized PSD, as shown in Fig. 2(b), with a combination of both $1/f^\alpha$ and Lorentzian components, given as [65]

$$\frac{S_V(f)}{V^2} = \frac{A}{f^\alpha} + \frac{Bf_c}{f^2 + f_c^2} \tag{2}$$

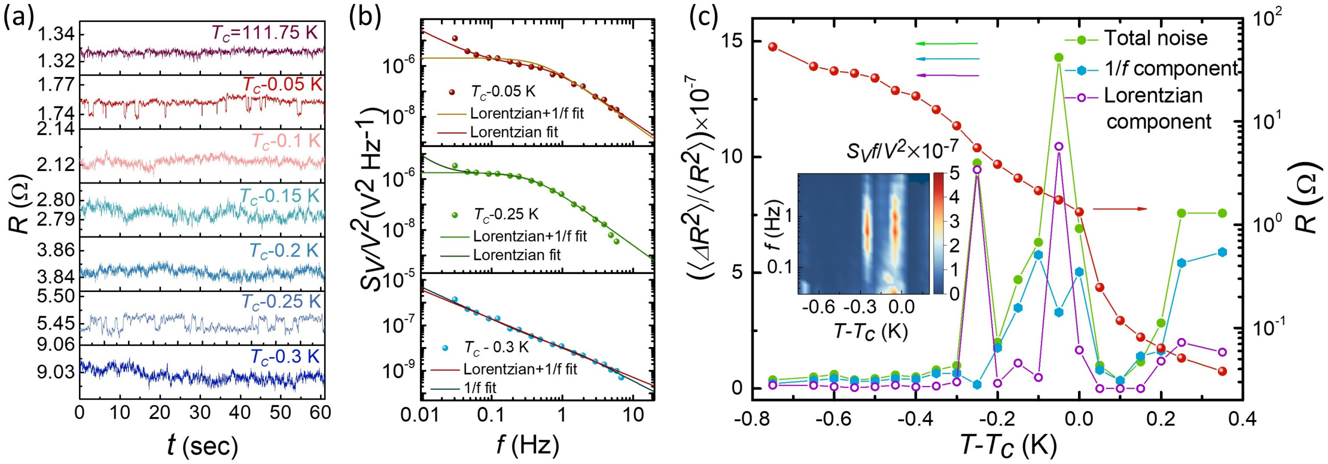

FIG. 2. Noise in $Ca_3(Ru_{0.9}Ti_{0.1})_2O_7$. (a). Resistance ($R$) as a function of time ($t$) from $T_c$ (111.75 K) to $T_c - 0.3$ K (111.45 K). Two level fluctuations are observed at $T_c - 0.05$ K and $T_c - 0.25$ K. (b) Normalized Power Spectral Density ($S_V(f)/V^2$) at $T_c - 0.05$ K, $T_c - 0.25$ K and $T_c - 0.3$ K. (c) Dependence of normalized variance ($\langle \Delta R^2 \rangle / \langle R^2 \rangle$) and resistance ($R$) on shifted temperature ($T - T_c$). Inset shows variation of $S_V f/V^2$ on $f$ and $T - T_c$.

where $A$ and $B$ represent the PSD due to $1/f^{\alpha}$ and Lorentzian components respectively, and $f_c$ is the corner frequency corresponding to the relaxation time of the Lorentzian. From the noise spectra shown in Fig. 2(b), it is evident that close to the transition there is a strong Lorentzian component as well as a significant $1/f^{\alpha}$ background, while away from the transition, $1/f^{\alpha}$ noise dominates.

The $T$-dependence of $\langle \Delta R^2 \rangle / \langle R^2 \rangle$, is shown in Fig. 2(c), along with the contributions from the narrowband Lorentzian and broadband $1/f^{\alpha}$ component ($\alpha \sim 1 - 1.4$, See SI Sec VII), which have been computed from the fitting parameters of Eq. [2] [65]. We observe two distinct peaks in $\langle \Delta R^2 \rangle / \langle R^2 \rangle$, at $T = 111.7$ K ($T_c - 0.05$ K) and $T = 111.5$ K ($T_c - 0.25$ K), where the Lorentzian component dominates. The Lorentzian component is maximum around $f_c \approx 0.1 - 0.5$ Hz (inset of Fig. 2(c)), which is consistent with the fitting parameters [See SI Sec. VII], implying a redistribution of the spectral weight and slowing down of electron kinetics across the transition. Appearance of TLF in our system is strongly indicative of an emergent collective phase with long range correlation that can occur across a phase transition, where the system becomes sensitive to one or very few fluctuators [65, 66]. In $Ca_3(Ru_xTi_{1-x})_2O_7$, MIT at $T_{MIT}$ is followed by a magnetic transition at $T_N$ ($T_N > T_{MIT}$) [36] for $x < 0.05$. With increased Ti doping ($x > 0.05$), we observe a single Mott transition as the intermediate metallic phase present at lower doping is unable to form a full percolative network [27], and average transport measurements are unable to resolve the two. However, we find low frequency noise to be extremely sensitive in resolving the two transitions, with the two distinct peaks in $1/f$ noise, and the appearance of the Lorentzian component at a temperature interval of $\sim 0.25$ K repeatable in multiple samples [See Sec. VI in SI].

To understand the electron kinetics that leads to $1/f^{\alpha}$ noise across the transition, we further studied the second spectrum ($s^{(2)}(f_2)$, $f_2$ being it's spectral frequency) [68], which is the fourth order statistics or kurtosis of the voltage noise. $s^{(2)}(f_2)$ is a measure of the correlation or non-Gaussianity of the fluctuations (purple trace in Fig. 3(a)) measured from the integrated noise indicated by $P_i \in [1, N]$ within a bandwidth $(f_l, f_H)$, as evaluated from $S_V(f)$ [See SI Sec. VIII]. The non-Gaussian component (NGC) in resistivity fluctuations has been employed as an extremely sensitive probe to the spectral wandering due to slow charge and spin kinetics, such as those in glasses [51]. In general, NGC indicates two possibilities, (a) percolative network of electrical conduction [26],and (b) long range correlation between the flucutators [22, 44]. The two cases can be distinguished from the spectral shape as $s^{(2)}(f_2)$ increases at low $f_2$ for correlation induced slowdown because the spectral weight is transferred to lower frequencies, while $s^{(2)}(f_2)$ remains frequency-independent in the case of percolation. In our samples, we find $s^{(2)}(f_2) \propto f_2^{-\beta}$ with $\beta \approx 0.2 - 0.5$ (Fig. 3(b)), at temperatures where $1/f^{\alpha}$ component is maximum (at the transition), indicating strong NGC and interactions between the fluctuators. The solid lines (Fig. 3 and Fig. 4(b)) represent fits to the data while dashed lines represent constant background expected for Gaussian fluctuations [See SI Sec. VIII] or uncorrelated fluctuators [26]. The $f_2$-dependence of $s^{(2)}(f_2)$ eliminates the possibility of additional $1/f^{\alpha}$ noise arising from classical percolation [69] or dynamical current redistribution (DCR) [70], which can arise at first order phase transition owing to the co-existence of phases, since the fluctuators are not correlated in this case. The frequency-dependence of $s^{(2)}(f_2)$ indicates that the correlation among $P_i$, which is a measure of the resistance fluctuations is non-zero, implying that the fluc-

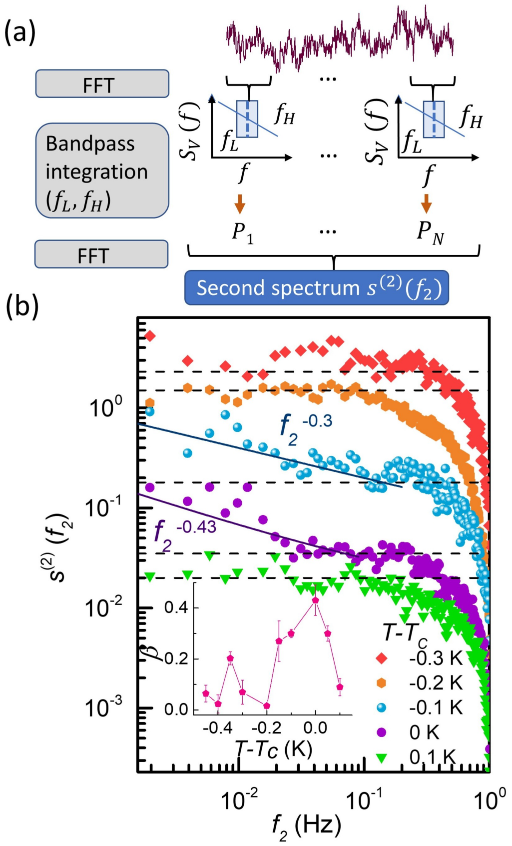

FIG. 3. Non Gaussianity in noise: (a). Schematic of second spectrum analysis. (b). Normalized second spectrum ($s^{(2)}(f_2)$) at different shifted temperatures ($T - T_c$), shifted vertically for clarity. Solid lines show the frequency dependence of $s^{(2)}(f_2) \propto f_2^{-\beta}$. Dashed lines are guide to the eye representing frequency independent background. Inset shows variation of exponent $\beta$ with $T - T_c$.

tuations are related between each time segment. This reveals the presence of "slow" relaxation time in the system, which represents "ergodicity breaking", a possible signature of glassy behavior [71–73] [See SI Sec. VIII and IX].

We repeated the noise measurements at $B = 50$ and 100 mT, applied parallel to the $a - b$ plane, which is higher than the field required to suppress the transition [27, 74]. The variation of $\langle \Delta R^2 \rangle / \langle R^2 \rangle$ with $T$ is shown in Fig. 4(a) ($T_c = 111.5$ K in this thermal cycle). The contributions from the Lorentzian and $1/f^\alpha$ components are computed separately for comparison. We observe complete suppression of the noise peak at lower $T$ while the peak at higher $T$, is partially suppressed. This indicates TLF to be arising from fluctuators with magnetic flavor. This can be modelled as fluctuations between two states separated by a finite energy barrier that is dependent on $B$. The system can switch between two metastable states with energy $E_i$ and $E_v$ by thermal activation (TA) [66] or by macroscopic quantum tunnelling (QMT) (inset of Fig. 4(a)) [75]. Within the framework of this model, a field-dependent energy barrier is given as $E_i(H) = E_0 + \Delta m_i \cdot H$, where $\Delta m_i = m_v - m_i$, $m_i$ and $m_v$ being the magnetic moment associated with the fluctuator in the states $i$ and $v$ respectively, and $H$ is the applied magnetic field. If $E_i$ changes even slightly, timescales associated with TLF being exponentially dependent [66, 75] also change significantly and goes beyond our experimental bandwidth. The peak in noise at lower $T$ possibly arises with the coherent switching of the "stripe" phase and G-AFM phase corresponding to MIT, while the peak at higher $T$ again comes with the emergence of the PM domain corresponding to Neel transition.

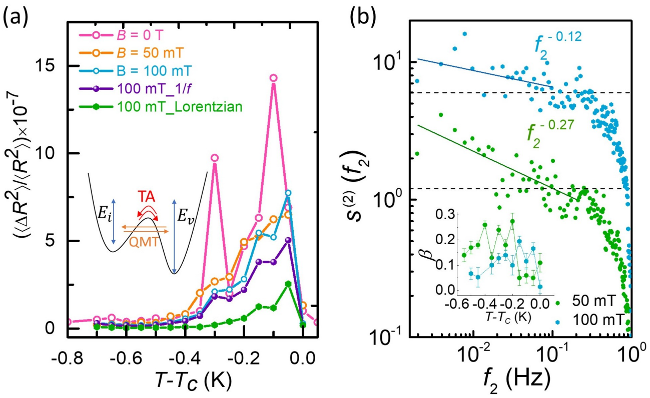

FIG. 4. Magnetic field dependence of noise. (a) Normalized variance ($\langle \Delta R^2 \rangle / \langle R^2 \rangle$) as a function of shifted temperature ($T - T_c$). Inset shows origin of TLF across an energy barrier. (b) Normalized second spectrum ($s^{(2)}(f_2)$) for $B = 100$ mT and 50 mT at T for maximum $\beta$, where $s^{(2)}(f_2) \propto f_2^{-\beta}$ shown by solid lines. Inset shows the variation of $\beta$ with $T - T_c$.

We also analyzed the second spectrum for $B = 50$ and 100 mT at $T - T_c = -0.05$ K where $1/f^\alpha$ noise is maximum (Fig. 4(b)). Crucially, we observe that compared to $B = 0$ case, the variation of $s^{(2)}(f_2)$ with $f_2$ is progressively weakened, as $B$ is increased from 50 mT to 100 mT, with $\beta$ varying between $0.05 - 0.3$ in the entire $T$ range (inset of Fig. 4(b)). We observe similar suppression for different thermal cycles [See SI Sec. X]), thereby strongly indicating the formation of spin-glass state near the transition.

Glassy electron kinetics, usually attributed to geometric frustration and quenched disorder, has been investigated close to MIT [20, 22, 76, 77]. We report an emerging spin-glass state for the first time near a first order Mott-MIT [27] at high $T$ of $\approx 110$ K without any geometric frustration in the system. The emergence of such a glassy state is not manifested in the $R - T$ of the sample [See SI Sec. XI]. Several possibilities of the origin of spin-glass formation exist. In case of RP materials such as $Sr_3MnTiO_7$, structural distortion of $MO_6$ octahedra and random distribution of $Mn^3/Mn^{4+}$ might be responsible for the observed spin glass behaviour [78]. In $Ca_4Mn_3O_{10}$, weak ferromagnetic clusters can arise from inhomogeneously distributed distortions of the crystallographic structure [79]. Spin glass phase has been predicted theoretically in $PrAu_2Si_2$ [80], which represents a system to achieve frustration with neither static disorder nor geometrically frustrated lattices, but through competing long range interactions. We believe in our case, spin-glass behavior can appear due to the distortion of the $RuO_6$ octeheadra due to the addition of Ti atoms as well as the presence of trace amounts of magnetic defects such as $Ru^{3+}/Ru^{5+}$. Such defects have been shown to give rise to spin-glass state in double perovskite ruthenates [81]. Another possibility is the frustration of competing interactions which gives rise to a “self-generated” glass phase [82]. Further investigation is necessary in this regard.

In conclusion, we have probed the Mott transition in $Ca_3(Ru_{0.9}Ti_{0.1})_2O_7$ with low frequency noise. We observe an increase in $1/f^{\alpha}$ noise by an order of magnitude across the transition. These slow fluctuation time scales originate from the glassy kinetics of the electrons close to the MIT, which is verified by the frequency dependence of the second spectrum. Magnetic field-dependent measurements indicate towards an intermittent spin glass formation which has not been previously observed across a first order Mott MIT.

SK acknowledges PMRF, SI and AG acknowledge MeitY for support. ZQM and YW acknowledge support of U.S. NSF through the Penn State 2DCC-MIP under NSF Cooperative Agreement No. DMR-2039351.

$^{\star}$Corresponding authors:
shreyak@iisc.ac.in
ski5160@psu.edu
$^{\dagger}$Present address: Department of Physics, Pennsylvania State University, University Park, Pennsylvania 16802, USA

---

[1] N. F. Mott, Proc. Phys. Soc. A **62**, 416 (1949).
[2] N. F. Mott, Rev. Mod. Phys. **40**, 677 (1968).
[3] M. Imada, A. Fujimori, and Y. Tokura, Rev. Mod. Phys. **70**, 1039 (1998).
[4] C.-M. Jian, Z. Bi, and C. Xu, Phys. Rev. B **96**, 115122 (2017).
[5] T. Furukawa, K. Miyagawa, H. Taniguchi, R. Kato, and K. Kanoda, Nature Physics **11**, 221 (2015).
[6] H. Terletska, J. Vučičević, D. Tanasković, and V. Dobrosavljević, Phys. Rev. Lett. **107**, 026401 (2011).
[7] T. Li, S. Jiang, L. Li, Y. Zhang, K. Kang, J. Zhu, K. Watanabe, T. Taniguchi, D. Chowdhury, L. Fu, *et al.*, Nature **597**, 350 (2021).
[8] P. Salev, L. Fratino, D. Sasaki, R. Berkoun, J. Del Valle, Y. Kalcheim, Y. Takamura, M. Rozenberg, and I. K. Schuller, Nature communications **12**, 1 (2021).
[9] S. Hormoz and S. Ramanathan, Solid-State Electronics **54**, 654 (2010).
[10] S. B. Roy, *Mott Insulators* (IOP publishing, 2019).
[11] S. Iqbal, L. T. Duy, H. Kang, R. Singh, M. Kumar, J. Park, and H. Seo, Advanced Functional Materials **31**, 2102567 (2021).
[12] Y. Wang, K.-M. Kang, M. Kim, H.-S. Lee, R. Waser, D. Wouters, R. Dittmann, J. J. Yang, and H.-H. Park, Materials Today **28**, 63 (2019).
[13] S. Zhang and G. Galli, npj Computational Materials **6**, 1 (2020).
[14] E. Abrahams, *50 Years Of Anderson Localization*, International journal of modern physics No. pt. 1 (World Scientific Publishing Company, 2010).
[15] N. Mott, *Metal-Insulator Transitions* (CRC Press, 2004).
[16] B. Spivak, S. V. Kravchenko, S. A. Kivelson, and X. P. A. Gao, Rev. Mod. Phys. **82**, 1743 (2010).
[17] E. Dagotto, Science **309**, 257 (2005).
[18] Y. Tokura and N. Nagaosa, Science **288**, 462 (2000).
[19] A. Hewson, *The Kondo Problem to Heavy Fermions*, Cambridge Studies in Magnetism (Cambridge University Press, 1997).
[20] V. Dobrosavljević, D. Tanasković, and A. A. Pastor, Phys. Rev. Lett. **90**, 016402 (2003).
[21] B. Hartmann, D. Zielke, J. Polzin, T. Sasaki, and J. Müller, Phys. Rev. Lett. **114**, 216403 (2015).
[22] S. Kar, A. K. Raychaudhuri, A. Ghosh, H. v. Löhneysen, and G. Weiss, Phys. Rev. Lett. **91**, 216603 (2003).
[23] S. c. v. Bogdanovich and D. Popović, Phys. Rev. Lett. **88**, 236401 (2002).
[24] Z. Topalian, S.-Y. Li, G. A. Niklasson, C. G. Granqvist, and L. B. Kish, Journal of Applied Physics **117**, 025303 (2015), https://doi.org/10.1063/1.4905739.
[25] V. Podzorov, M. Uehara, M. E. Gershenson, T. Y. Koo, and S.-W. Cheong, Phys. Rev. B **61**, R3784 (2000).
[26] A. Sahoo, S. D. Ha, S. Ramanathan, and A. Ghosh, Phys. Rev. B **90**, 085116 (2014).
[27] J. Peng, X. Ke, G. Wang, J. E. Ortmann, D. Fobes, T. Hong, W. Tian, X. Wu, and Z. Q. Mao, Phys. Rev. B **87**, 085125 (2013).
[28] I. B. Sharma and D. Singh, Bull Mater Sci **21**, 363 (1998).
[29] Y. Maeno et.al, Nature **372**, 532 (1994).
[30] A. J. Leggett and Y. Liu, Journal of Superconductivity and Novel Magnetism **34**, 1647 (2021).
[31] S. A. Grigera, R. S. Perry, A. J. Schofield, M. Chiao, S. R. Julian, G. G. Lonzarich, S. I. Ikeda, Y. Maeno, A. J. Millis, and A. P. Mackenzie, Science **294**, 329 (2001).
[32] S. Nakatsuji, D. Hall, L. Balicas, Z. Fisk, K. Sugahara, M. Yoshioka, and Y. Maeno, Phys. Rev. Lett. **90**, 137202 (2003).
[33] J. M. Longo, P. M. Raccah, and J. B. Goodenough, Nature **39**, 1327 (1968).
[34] S. Nakatsuji, S.-i. Ikeda, and Y. Maeno, J. Phys. Soc. Jpn. **66**, 1868 (1997).
[35] T. He and R. J. Cava, Phys. Rev. B **63**, 172403 (2001).
[36] G. Cao, S. McCall, J. E. Crow, and R. P. Guertin, Phys. Rev. Lett. **78**, 1751 (1997).
[37] F. Baumberger, N. J. C. Ingle, N. Kikugawa, M. A. Hossain, W. Meevasana, R. S. Perry, K. M. Shen, D. H. Lu, A. Damascelli, A. Rost, A. P. Mackenzie, Z. Hussain, and Z.-X. Shen, Phys. Rev. Lett. **96**, 107601 (2006).
[38] X. Ke, J. Peng, D. J. Singh, T. Hong, W. Tian, C. R. Dela Cruz, and Z. Q. Mao, Phys. Rev. B **84**, 201102 (2011).
[39] A. Gangshettiwar, Y. Zhu, Z. Jiang, J. Peng, Y. Wang, J. He, J. Zhou, Z. Mao, and K. Lai, Phys. Rev. B **101**,

201106 (2020).

[40] P. G. Radaelli, R. M. Ibberson, D. N. Argyriou, H. Casalta, K. H. Andersen, S.-W. Cheong, and J. F. Mitchell, Phys. Rev. B **63**, 172419 (2001).

[41] P. Dutta and P. M. Horn, Rev. Mod. Phys. **53**, 497 (1981).

[42] H. K. Kundu, S. Ray, K. Dolui, V. Bagwe, P. R. Choudhury, S. B. Krupanidhi, T. Das, P. Raychaudhuri, and A. Bid, Phys. Rev. Lett. **119**, 226802 (2017).

[43] S. Kundu, T. Bar, R. K. Nayak, and B. Bansal, Phys. Rev. Lett. **124**, 095703 (2020).

[44] U. Chandni, A. Ghosh, H. S. Vijaya, and S. Mohan, Phys. Rev. Lett. **102**, 025701 (2009).

[45] S. Islam, S. Shamim, and A. Ghosh, Advanced Materials , 2109671 (2022).

[46] A. Ghosh, S. Kar, A. Bid, and A. Raychaudhuri, arXiv **58** (2004), https://arxiv.org/abs/cond-mat/0402130v1.

[47] S. Bhattacharyya, M. Banerjee, H. Nhalil, S. Islam, C. Dasgupta, S. Elizabeth, and A. Ghosh, ACS Nano **9**, 12529 (2015).

[48] S. Islam, S. Bhattacharyya, A. Kandala, A. Richardella, N. Samarth, and A. Ghosh, Appl. Phys. Lett **111**, 062107 (2017).

[49] F. Hooge, Physics Letters A **29**, 139 (1969).

[50] J. H. Scofield, J. V. Mantese, and W. W. Webb, Phys. Rev. B **32**, 736 (1985).

[51] M. B. Weissman, Rev. Mod. Phys. **60**, 537 (1988).

[52] A. N. Pal and A. Ghosh, Appl. Phys. Lett **95**, 082105 (2009).

[53] V. K. Sangwan, H. N. Arnold, D. Jariwala, T. J. Marks, L. J. Lauhon, and M. C. Hersam, Nano Lett. **13**, 4351 (2013).

[54] A. N. Pal, S. Ghatak, V. Kochat, E. S. Sneha, A. Sampathkumar, S. Raghavan, and A. Ghosh, ACS Nano **5**, 2075 (2011).

[55] P. Karnatak, T. P. Sai, S. Goswami, S. Ghatak, S. Kaushal, and A. Ghosh, Nat Commun **7**, 1 (2016).

[56] S. Kakkar, P. Karnatak, M. A. Aamir, K. Watanabe, T. Taniguchi, and A. Ghosh, Nanoscale **12**, 17762 (2020).

[57] P. Karnatak, T. Paul, S. Islam, and A. Ghosh, Advances in Physics: X **2**, 428 (2017).

[58] S. Shamim, S. Mahapatra, C. Polley, M. Y. Simmons, and A. Ghosh, Phys. Rev. B **83**, 233304 (2011).

[59] A. N. Pal and A. Ghosh, Phys. Rev. Lett. **102**, 126805 (2009).

[60] A. Ghosh and A. K. Raychaudhuri, Phys. Rev. Lett. **84**, 4681 (2000).

[61] O. Cohen and Z. Ovadyahu, Phys. Rev. B **50**, 10442 (1994).

[62] B. R. Conrad, W. G. Cullen, W. Yan, and E. D. Williams, Applied Physics Letters **91**, 242110 (2007), https://doi.org/10.1063/1.2823577.

[63] Z. Li, M. Sotto, F. Liu, M. K. Husain, H. Yoshimoto, Y. Sasago, D. Hisamoto, I. Tomita, Y. Tsuchiya, and S. Saito, Scientific reports **8**, 1 (2018).

[64] X. Li, T. Zanotti, T. Wang, K. Zhu, F. M. Puglisi, and M. Lanza, Adv. Funct. Mater. , 2102172 (2021).

[65] A. Bid, A. Guha, and A. K. Raychaudhuri, Phys. Rev. B **67**, 174415 (2003).

[66] B. Raquet, A. Anane, S. Wirth, P. Xiong, and S. von Molnár, Phys. Rev. Lett. **84**, 4485 (2000).

[67] P. Dutta, P. Dimon, and P. M. Horn, Phys. Rev. Lett. **43**, 646 (1979).

[68] G. T. Seidler and S. A. Solin, Phys. Rev. B **53**, 9753 (1996).

[69] R. H. Koch, R. B. Laibowitz, E. I. Alessandrini, and J. M. Viggiano, Phys. Rev. B **32**, 6932 (1985).

[70] G. T. Seidler, S. A. Solin, and A. C. Marley, Phys. Rev. Lett. **76**, 3049 (1996).

[71] Z. Kutnjak, C. Filipič, R. Pirc, A. Levstik, R. Farhi, and M. El Marssi, Physical Review B **59**, 294 (1999).

[72] L. F. Cugliandolo, J. Kurchan, P. Le Doussal, and L. Peliti, Physical review letters **78**, 350 (1997).

[73] G. Carleo, F. Becca, M. Schiró, and M. Fabrizio, Scientific reports **2**, 1 (2012).

[74] M. Zhu, J. Peng, T. Zou, K. Prokes, S. D. Mahanti, T. Hong, Z. Q. Mao, G. Q. Liu, and X. Ke, Phys. Rev. Lett. **116**, 216401 (2016).

[75] L.-D. Chang and S. Chakravarty, Phys. Rev. B **29**, 130 (1984).

[76] J. Jaroszyński, D. Popović, and T. Klapwijk, Physica E **12**, 612 (2002), proceedings of the Fourteenth International Conference on the Electronic Properties of Two-Dimensional Systems.

[77] J. Brandenburg, J. Müller, and J. A. Schlueter, New J. Phys. **14**, 023033 (2012).

[78] T. Nan, S. Emori, C. T. Boone, X. Wang, T. M. Oxholm, J. G. Jones, B. M. Howe, G. J. Brown, and N. X. Sun, Phys. Rev. B **91**, 214416 (2015).

[79] J. Lago, P. D. Battle, and M. J. Rosseinsky, Journal of Physics: Condensed Matter **12**, 2505 (2000).

[80] E. Goremychkin, R. Osborn, B. Rainford, R. Macaluso, D. Adroja, and M. Koza, Nature Physics **4**, 766 (2008).

[81] H. Yatsuzuka, Y. Haraguchi, A. Matsuo, K. Kindo, and H. A. Katori, Scientific Reports **12**, 1 (2022).

[82] J. Schmalian and P. G. Wolynes, Phys. Rev. Lett. **85**, 836 (2000).